

Nanoparticle iron-phosphate anode material for Li-ion battery

Dongyeon Son

School of Materials Science and Engineering, and Research Center for Energy Conversion and Storage, Seoul National University, Seoul, Korea

Eunjin Kim

Department of Applied Chemistry, Kumoh National Institute of Technology, Gumi, Korea

Tae-Gon Kim

School of Materials Science and Engineering, and Research Center for Energy Conversion and Storage, Seoul National University, Seoul, Korea

Min Gyu Kim

Beamline Research Division, Pohang Accelerator Laboratory, Pohang University of Science and Technology, Pohang, Korea

Jaephil Cho

Department of Applied Chemistry, Kumoh National Institute of Technology, Gumi, Korea

Byungwoo Park^{a)}

School of Materials Science and Engineering, and Research Center for Energy Conversion and Storage, Seoul National University, Seoul, Korea

(Received 17 August 2004; accepted 20 October 2004)

Nanoparticle crystalline iron phosphates ($\text{FePO}_4 \cdot 2\text{H}_2\text{O}$ and FePO_4) were synthesized using a (CTAB) surfactant as an anode material for Li rechargeable batteries. The electrochemical properties of the nanoparticle iron phosphates were characterized with a voltage window of 2.4–0 V. A variscite orthorhombic $\text{FePO}_4 \cdot 2\text{H}_2\text{O}$ showed a large initial charge capacity of 609 mAh/g. On the other hand, a tridymite triclinic FePO_4 exhibited excellent cyclability: the capacity retention up to 30 cycles was $\sim 80\%$, from 485 to 375 mAh/g. The iron phosphate anodes exhibited the highest reported capacity, while the cathode LiFePO_4 has an ideal capacity of 170 mAh/g. © 2004 American Institute of Physics. [DOI: 10.1063/1.1835995]

Since the introduction of commercial lithium-ion batteries for portable devices in the 1990s, the development of new anode materials is essential for improving the energy density.¹ The graphite generally used in lithium rechargeable batteries has a capacity of 372 mAh/g. These capacity limitations have inspired researchers to find alternative anode materials. Li–Sn alloy has been studied due to its high capacity compared to commercial graphite.^{2–4} However, Sn–metal anode has a problem with severe capacity fading due to structural instability related to large volume changes.

Iron phosphates have been explored as cathode materials only.^{5,6} Padhi *et al.* reported an olivine-type LiFePO_4 cathode, which has a theoretical capacity of 170 mAh/g. As lithium is intercalated/deintercalated from the octahedral sites, olivine-type LiFePO_4 has a flat voltage plateau at 3.4 V versus Li. In addition, iron phosphates exhibited different types of structures depending on the synthesis conditions. For instance, FePO_4 showed a trigonal structure at normal pressure, but converted to orthorhombic structure at high pressure.⁷ More recently, Song *et al.*⁸ and Reale *et al.*⁹ reported monoclinic (with a space group $P2_1/n$), orthorhombic (with $Pbca$), or hexagonal (with $P6_3mc$) FePO_4 . These iron phosphates exhibited an open circuit voltage of approximately 4 V, and showed a voltage plateau at ~ 3 V (working as cathodes) with discharge capacities below 100 mAh/g.

We report here a possibility of iron phosphates as anode materials for Li rechargeable batteries. Despite iron phos-

phates being briskly investigated as a positive electrode, the anode materials of FePO_4 have not been reported. The capacity of synthesized nanoparticle iron phosphates is approximately three times higher than the ideal capacity of the LiFePO_4 cathode.

The $\text{FePO}_4 \cdot 2\text{H}_2\text{O}$ was fabricated by using a cationic surfactant, cetyl-trimethyl-ammonium bromide (CTAB). The CTAB surfactant (1.4 g) was added to distilled water (20 ml) and stirred for 30 min. Then, $\text{FeCl}_3 \cdot 6\text{H}_2\text{O}$ (3 g) and H_3PO_4 (6.5 g) were gradually added to the solution, and stirred until they were completely dissolved. Subsequently, the suspensions were aged at 90 °C for a week in an oven. The resultant was then washed with de-ionized water, filtered off, and dried at 100 °C for 4 h. The tridymite FePO_4 was obtained from dehydration of $\text{FePO}_4 \cdot 2\text{H}_2\text{O}$ at 400 °C annealing for 8 h in a furnace.

The electrode composition was iron-phosphate anode : binder : carbon black in a weight ratio of 3 : 1 : 1. A slurry was then prepared by mixing them with a *N*-methyl-2-pyrrolidone (NMP) solution. The coin-type half cells (2016 size) prepared in an argon-filled glove box contained an iron-phosphate anode, a Li metal counter electrode, and a microporous polyethylene separator. The electrolyte used was 1 M LiPF_6 with ethylene carbonate/diethylene carbonate/ethylmethyl carbonate (EC/DEC/EMC). The cycle life of the cells was performed at a rate of 61 mA/g for $\text{FePO}_4 \cdot 2\text{H}_2\text{O}$, and 49 mA/g for FePO_4 between a voltage window of 2.4 and 0 V. Note that open circuit voltages of our samples were around 2 V. For the XRD measurements, the cells were dis-

^{a)}Electronic mail: byungwoo@snu.ac.kr

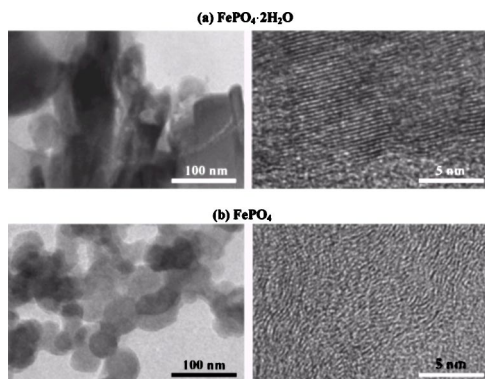


FIG. 1. High-resolution TEM images of the iron phosphates: (a) as-synthesized $\text{FePO}_4 \cdot 2\text{H}_2\text{O}$, and (b) FePO_4 (annealed at 400°C for 8 h).

assembled in a glove box (H_2O level < 50 ppm), and the cycled iron-phosphate powders were rinsed thoroughly with a DMC solution to remove any LiPF_6 salts.

As shown in Fig. 1, transmission electron microscopy (TEM) was used to identify the microstructures of the iron phosphates. The average nanoparticle size confirmed by TEM is approximately 100 nm for $\text{FePO}_4 \cdot 2\text{H}_2\text{O}$, and ~ 50 nm for FePO_4 . These are in good agreement with the x-ray diffraction patterns shown in Fig. 2. The size estimated from the Scherrer formula of Δk versus k (the scattering vector) was a few hundred nanometers for $\text{FePO}_4 \cdot 2\text{H}_2\text{O}$, and ~ 40 nm for FePO_4 . Interestingly, a high-resolution TEM shows that both orthorhombic $\text{FePO}_4 \cdot 2\text{H}_2\text{O}$ and triclinic FePO_4 have a nanostructured periodicity (~ 0.3 nm). This curling-shaped nano-periodicity was also observed in carbon, WS_2 , Ga_2O_3 , V_2O_5 , etc.^{10–15} More detailed studies of the role of nanostructures on the electrochemical properties are currently underway. Amorphous iron-phosphate anodes showed a rapid capacity decay, thus showing less than

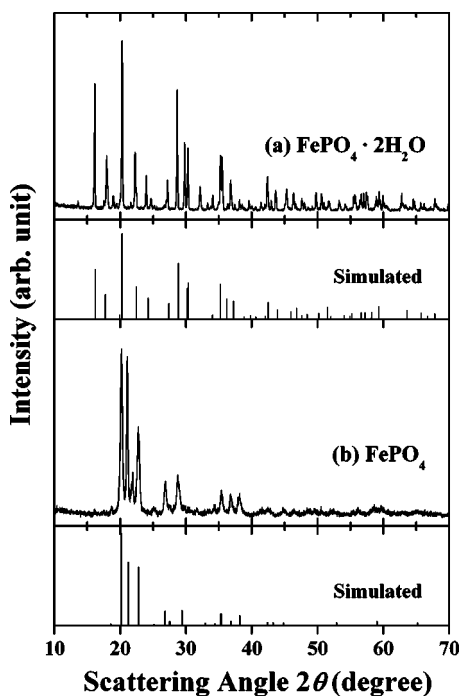


FIG. 2. Measured and simulated x-ray diffraction patterns of (a) as-synthesized $\text{FePO}_4 \cdot 2\text{H}_2\text{O}$, and (b) FePO_4 (annealed at 400°C for 8 h).

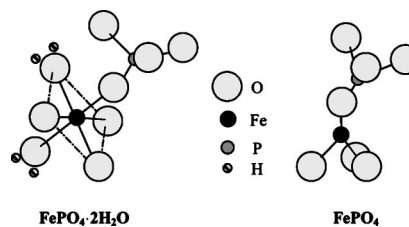


FIG. 3. Schematic representation of the basic crystal structures of iron phosphates: the variscite orthorhombic ($Pbca$) $\text{FePO}_4 \cdot 2\text{H}_2\text{O}$ and tridymite triclinic ($P1$) FePO_4 .

100 mAh/g after 10 cycles, even with a similar initial-charge capacity.¹⁶

The crystal structure of the as-synthesized iron phosphate was very similar to the one reported in the literature for the variscite $\text{AlPO}_4 \cdot 2\text{H}_2\text{O}$ or $\text{GaPO}_4 \cdot 2\text{H}_2\text{O}$.^{17,18} Using the simulation technique (ATOMS¹⁹) after replacing Al with Fe, the crystal structure of the as-prepared iron phosphate was identified as an orthorhombic $\text{FePO}_4 \cdot 2\text{H}_2\text{O}$, which is a variscite structure with the space group $Pbca$ [Fig. 2(a)], with lattice parameters of $a=0.9926$ nm, $b=0.8619$ nm, and $c=0.9976$ nm. After annealing at 400°C for 8 h, the water molecules in $\text{FePO}_4 \cdot 2\text{H}_2\text{O}$ were successfully removed, and the XRD data of Fig. 2(b) confirmed a triclinic FePO_4 phase, which has a space group $P1$ with $a=1.0163$ nm, $b=1.7624$ nm, $c=8.3733$ nm, and $\alpha=90.01^\circ$, $\beta=90.03^\circ$, $\gamma=89.98^\circ$. The schematic figures of the variscite $\text{FePO}_4 \cdot 2\text{H}_2\text{O}$ and tridymite FePO_4 are shown in Fig. 3.

To investigate the superior electrochemical properties of iron phosphates, coin-type half cells were cycled in extreme conditions, between 2.4 and 0 V.^{20–22} Analogous tin-phosphate anode showed severe capacity fading even between 1.5 and 0 V, and getting much worse with higher cut-off voltages.¹ Figure 4 shows the voltage profiles and capacity retention of the variscite $\text{FePO}_4 \cdot 2\text{H}_2\text{O}$ and the

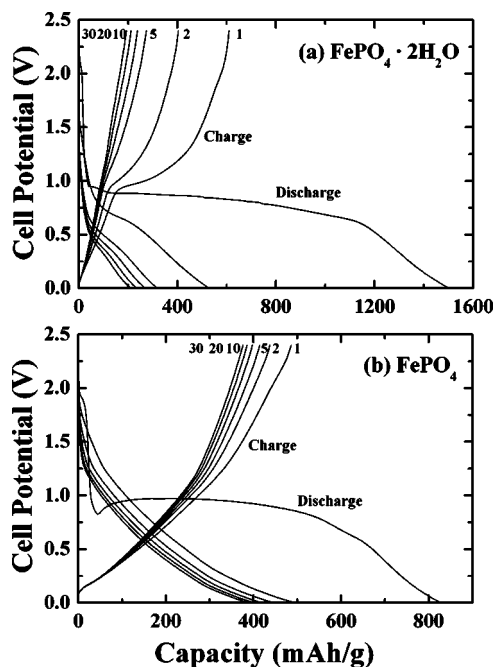


FIG. 4. Voltage profiles of the iron phosphates between 2.4 and 0 V. The cells were cycled at (a) 61 mA/g for variscite $\text{FePO}_4 \cdot 2\text{H}_2\text{O}$ (initial capacity of 609 mAh/g), and (b) 49 mA/g for tridymite FePO_4 (initial capacity of 485 mAh/g).

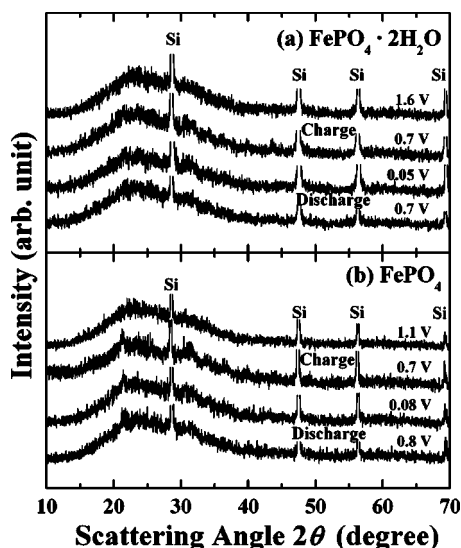


FIG. 5. XRD patterns of (a) the cycled $\text{FePO}_4 \cdot 2\text{H}_2\text{O}$ and (b) cycled FePO_4 , during the first discharge and charge at a specific voltage.

tridymite FePO_4 . The initial charge capacity of the $\text{FePO}_4 \cdot 2\text{H}_2\text{O}$ is high (609 mAh/g), but the capacity faded noticeably during cycling. In contrast, the tridymite FePO_4 had an initial charge capacity of 485 mAh/g, which is approximately three times higher than the ideal capacity of cathode LiFePO_4 . In addition, the capacity retention [Fig. 4(b)] at a rate of 49 mA/g up to 30 cycles was $\sim 80\%$ (from 485 to 375 mAh/g). It should be noted that the irreversible capacity of the variscite $\text{FePO}_4 \cdot 2\text{H}_2\text{O}$ anode (~ 897 mAh/g) is larger than the tridymite FePO_4 (~ 344 mAh/g), which is probably due to the side reactions with both the H_2O molecules and residual surfactants.

The electrochemical reactions of cathode LiFePO_4 involved the $\text{Fe}^{3+}/\text{Fe}^{2+}$ redox coupling. Therefore, the theoretical capacity of the LiFePO_4 cathode is only 170 mAh/g. However, iron-phosphate anodes can have a high capacity, probably due to the $\text{Fe}^{3+}/\text{Fe}^{2+}/\text{Fe}^0$ redox reactions. Poizot *et al.*²³ reported that the $3d$ transition-metal oxides could be reversibly reduced and oxidized, coupled with the formation/destruction of Li_2O , with the formation of a nanoparticle $3d$ transition metal. Analogous reactions may apply to iron phosphates, and more detailed experiments (Mössbauer, XANES, etc.) are currently underway to identify the reaction mechanisms. To confirm the phases during discharging/charging, the XRD patterns of both $\text{FePO}_4 \cdot 2\text{H}_2\text{O}$ and FePO_4 were investigated (Fig. 5). As the anode was discharged (lithiated) to 0 V, the crystalline peaks of the $\text{FePO}_4 \cdot 2\text{H}_2\text{O}$ and FePO_4 disappeared, indicating an amorphous or nanocrystalline state.

In conclusion, nanoparticle iron phosphates ($\text{FePO}_4 \cdot 2\text{H}_2\text{O}$ and FePO_4) were achieved using a CTAB surfactant as a new anode material for Li rechargeable batteries. The synthesized triclinic iron phosphate exhibited excellent cyclability: the capacity retention up to 30 cycles was $\sim 80\%$, from 485 to 375 mAh/g. Also, the capacity is approximately three times higher than the ideal value of cathode LiFePO_4 . This original nanoparticle iron phosphate demonstrates a potential for use as Li battery anode materials.

The authors thank Chunjoong Kim for the TEM measurements. This work was supported by the National R&D Program of the Ministry of Science and Technology, the Basic Research Program (R01-2004-000-10173-0) of KOSEF, the Ministry of Information and Communication (MIC) in Korea, and KOSEF through the Research Center for Energy Conversion and Storage at Seoul National University.

- ¹Y. Idota, T. Kubota, A. Matsufuji, Y. Maekawa, and T. Miyasaka, *Science* **276**, 1395 (1997).
- ²D. Aurbach, A. Nimberger, B. Markovsky, E. Levi, E. Sominski, and A. Gedanken, *Chem. Mater.* **14**, 4155 (2002).
- ³I. A. Courtney and J. R. Dahn, *J. Electrochem. Soc.* **144**, 2943 (1997).
- ⁴J.-M. Tarascon and M. Armand, *Nature (London)* **414**, 359 (2001).
- ⁵A. K. Padhi, K. S. Nanjundaswamy, and J. B. Goodenough, *J. Electrochem. Soc.* **144**, 1188 (1997).
- ⁶S.-Y. Chung, J. T. Blocking, and Y.-M. Chiang, *Nat. Mater.* **1**, 123 (2002).
- ⁷M. P. Pasternak, G. K. Rozenberg, A. P. Milner, M. Amanowicz, U. Schwaetz, K. Syassen, R. D. Taylor, M. Hanfland, and K. Brister, *Phys. Rev. Lett.* **79**, 4409 (1997).
- ⁸Y. Song, P. Y. Zavalij, M. Suzuki, and M. S. Whittingham, *Inorg. Chem.* **41**, 5778 (2002).
- ⁹P. Reale, B. Scrosati, C. Delacourt, C. Wurm, M. Morcrette, and C. Masquelier, *Chem. Mater.* **15**, 5051 (2003).
- ¹⁰T. Hyeon, S. Han, Y.-E. Sung, K.-W. Park, and Y.-W. Kim, *Angew. Chem., Int. Ed.* **42**, 4352 (2003).
- ¹¹T.-W. Kim, I.-S. Park, and R. Ryoo, *Angew. Chem., Int. Ed.* **42**, 4375 (2003).
- ¹²Y. D. Li, X. L. Li, R. R. He, J. Zhu, and Z. X. Deng, *J. Am. Chem. Soc.* **124**, 1411 (2002).
- ¹³U. M. Graham, S. Sharma, M. K. Sunkara, and B. H. Davis, *Adv. Funct. Mater.* **13**, 576 (2003).
- ¹⁴M. E. Sphar, P. Bitterli, R. Nesper, M. Muller, F. Krumeich, and H. U. Nissen, *Angew. Chem., Int. Ed.* **37**, 1263 (1998).
- ¹⁵G. R. Ratzke, F. Krumeich, and R. Nesper, *Angew. Chem., Int. Ed.* **41**, 2447 (2002).
- ¹⁶J. Cho, D. Son, and B. Park (unpublished).
- ¹⁷A. M. Beale and G. Sankar, *J. Mater. Chem.* **12**, 3064 (2002).
- ¹⁸H. Graetsch, *Acta Crystallogr., Sect. C: Cryst. Struct. Commun.* **56**, 401 (2000).
- ¹⁹E. Dowty, *ATOMS. Shape software*, 521 Hidden Valley Road, Kingsport, Tennessee, 2002.
- ²⁰Y. J. Kim, H. Kim, B. Kim, D. Ahn, J.-G. Lee, T.-J. Kim, D. Son, J. Cho, Y.-W. Kim, and B. Park, *Chem. Mater.* **15**, 1505 (2003).
- ²¹J. Cho, Y. J. Kim, T.-J. Kim, and B. Park, *Angew. Chem., Int. Ed.* **40**, 3367 (2001).
- ²²J. Cho, Y.-W. Kim, B. Kim, J.-G. Lee, and B. Park, *Angew. Chem., Int. Ed.* **42**, 1618 (2003).
- ²³P. Poizot, S. Laruelle, S. Grugeon, L. Dupont, and J.-M. Tarascon, *Nature (London)* **407**, 496 (2000).